GEODYNAMICS & TECTONOPHYSICS
Published by the Institute of the Earth's Crust, Siberian Branch, Russian Academy of Sciences

PALEOGEODYNAMICS

2023 VOLUME 14 ISSUE 6 ARTICLE 0729

ISSN 2078-502X

DOI: 10.5800/GT-2023-14-6-0729

A MODEL OF THE LATE MESOZOIC AND CENOZOIC THERMOTECTONIC EVOLUTION OF THE PRE-MESOZOIC BASEMENT ROCKS IN SOUTH TUVA

E.V. Vetrov ✉, N.I. Vetrova

Sobolev Institute of Geology and Mineralogy, Siberian Branch of the Russian Academy of Sciences, 3 Academician Koptyug Ave, Novosibirsk 630090, Russia

ABSTRACT. Thermotectonic modeling was performed for the crystalline rocks of South Tuva using the apatite fission-track analysis. Thermotectonic modeling made it possible to visualize the Late Mesozoic and Cenozoic cooling history of the Pre-Mesozoic basement rocks, and to reconstruct the chronology and scale of the denudational processes over the last 125 myr and the evolution of paleorelief of South Tuva over the last 100 myr. The modeling results depicted several Mesozoic-Cenozoic episodes of cooling due to differential denudation and exhumation of the Pre-Mesozoic basement rocks. A differential denudation is related to an asynchronous activation of fault structures controlling the tectonic evolution of South Tuva. It is shown that the Early Cretaceous (~125–100 Ma) activation of the Agar-Dag-Oka thrust fault zone could result from the post-collisional processes after the collision between Siberia and Amuria and/or consecutive collision between the Cimmerian blocks. An intense activation of the Agar-Dag-Oka fault zone in the Late Cretaceous (~100–75 Ma), accompanied by significant basement rock exhumation in the eastern South Tuva to absolute heights of 1200 m, could be caused by the Karakoram-Pamir collision in the south of Eurasia. The Late Cenozoic (25–0 Ma) activation of the main fault zones of South Tuva represents a far-field effect of the Indo-European collision on the southern Eurasian continent. At the same time, there were the maximum basement uplift in the junction zone between the South Tannuola and Ubsunur-Bii-Khem fault zones and the transformation of relief of South Tuva from moderately dissected, with absolute heights of 500 to 1400 m, to modern, with absolute heights of 800 to 2600 m.

KEYWORDS: Tuva; Central Asian fold belt; apatite fission-track analysis; modeling; Mesozoic; Cenozoic

FUNDING: The study was carried out as part of the Grant of the President of the Russian Federation МК-3510.2022.1.5 and that of the state assignment of the IGM SB RAS 122041400214-9.

RESEARCH ARTICLE

Correspondence: Evgeny V. Vetrov, vetrov@igm.nsc.ru

Received: April 12, 2023
Revised: May 23, 2023
Accepted: June 14, 2023

FOR CITATION: Vetrov E.V., Vetrova N.I., 2023. A Model of the Late Mesozoic and Cenozoic Thermotectonic Evolution of the Pre-Mesozoic Basement Rocks in South Tuva. Geodynamics & Tectonophysics 14 (6), 0729. doi:10.5800/GT-2023-14-6-0729

1. INTRODUCTION

The study of tectonic stages in the development of the Central Asian Fold Belt (CAFB) is an essential aspect for understanding a long-term evolution of orogens. The CAFB, located between the cratons of North China, Tarim, Siberia and Baltica, is the largest orogen in the world [Sengör et al., 1993; Windley et al., 2007]. Its structure represents a complex collage consisting of terrains of various geodynamic nature (island-arc, collisional, intraplate), overlapped in result of the closure of different Paleo-Asian oceanic branches and the Paleozoic accretionary-collisional events [Dobretsov, 2003; Buslov et al., 2004, 2013; Windley et al., 2007; Wilhem et al., 2012; Xiao et al., 2013]. It is considered that the final closure of the Paleo-Asian Ocean occurred in the Late Paleozoic [Didenko et al., 1994; Buslov, 2011, 2014] and was accompanied by collisional and/or post-collisional tectonomagmatic activity [Wang et al., 2009; Wilhem et al., 2012; Vetrov et al., 2021a]. After the Paleozoic assembling, the different segments of the CAFB were reactivated during the Mesozoic and Cenozoic as a result of tectonic events at the southern and southeastern margins of the Eurasian continent [Molnar, Tapponnier, 1975; Dobretsov et al., 1996]. A large-scale reactivation of the CAFB structures caused a deformation of the upper continental crust and the formation of intracontinental mountain ranges, intermountain depressions and basins filled with the Mesozoic and Cenozoic sedimentary deposits. The sedimentary record preserved in intermountain depressions and basins gives an implication of the character of tectonic regime at that time. A full understanding of the Mesozoic-Cenozoic tectonic evolution of different segments of the CAFB is impossible without using precision methods. One of such methods capable of providing information on the Mesozoic and Cenozoic tectonic processes in the upper crust is apatite fission-track analysis. The present paper presents the results of a study of the thermotectonic evolution of basement rocks of one of the northern segments of the CAFB (Fig. 1) – South Tuva. The Pre-Mesozoic basement of South Tuva was largely formed during the Late Proterozoic – Early Paleozoic accretionary-collisional events [Zonenshayn et al., 1990; Berzin, Kungurtsev, 1996; Dobretsov et al., 2003; Gordienko, 2004, 2019; Vladimirov et al., 2005; Dobretsov, Buslov, 2007; Vetrov et al., 2019]. Its further tectonic evolution is related to multiple reactivations of large fault structures, such as South Tannuola, Ubsunur–Bii-Khem and Agar-Dag–Oka fault zones (Fig. 2) [Vetrov et al., 2020]. Modern earthquakes with a magnitude of up to 7 [Ovsyuchenko, Butanayev, 2017] imply that the faults in the study area are active and still control neotectonic evolution of the Tannuola range and the Sangilen upland.

The Proterozoic-Paleozoic rocks of South Tuva are overlain by the Mesozoic and Cenozoic deposits though the preserved sedimentary record shows the character of tectonic regime for only a limited time interval, and numerous questions concerning the stages of the Pre-Mesozoic basement growth and denudation remain open. In this connection, thermotectonic modeling was performed based on the apatite fission-track analysis data [De Grave et al., 2014; Vetrov et al., 2022] for the crystalline rocks of South Tuva. The aim of the study is to visualize the Late Mesozoic – Cenozoic cooling history of the Pre-Mesozoic basement rocks of South Tuva, chronology and scale of denudational processes, and to reconstruct the evolution of the paleorelief over the last 100 Ma.

2. THERMOTECTONIC MODELING TECHNIQUE

The thermotectonic modeling strategy was earlier described in detail in [Vetrov, 2016]. This study involved a similar technique exemplified by another object within the CAFB. The apatite fission-track (AFT) analysis is one

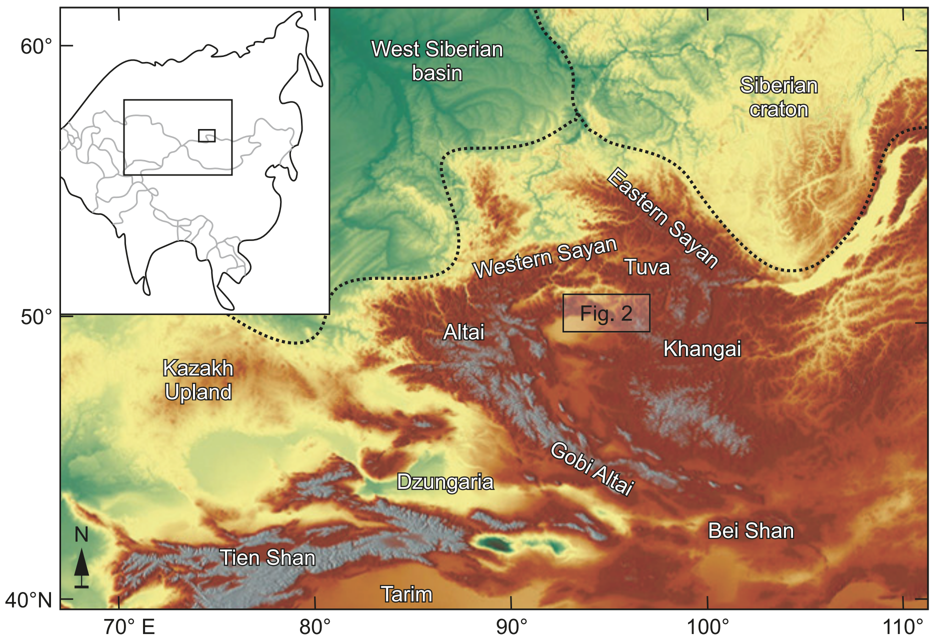

Fig. 1. Location of the study area in the northern part of the CAFB.

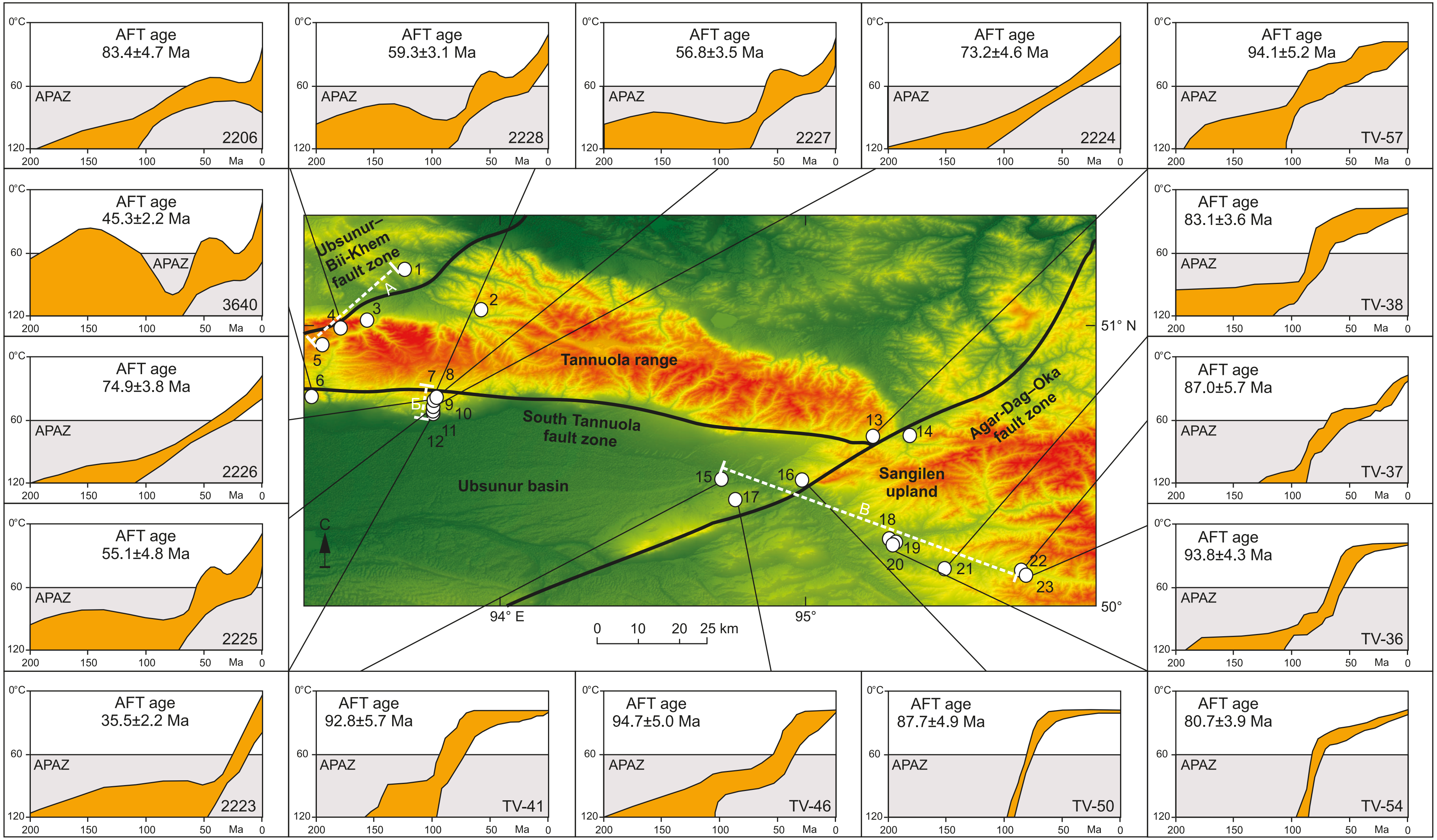

Fig. 2. The main fault zones of South Tuva and the results of AFT dating after [De Grave et al., 2014; Vetrov et al., 2022]. The sample numbers shown on the map are consistent with the serial numbers in Table 1.

Table 1. Sampling sites, lithology, and fission-track parameters

№	Sample	Coordinates		Height, m	Sampling site	Lithology	AFT age, Ma	Mean track length, μm
		Latitude	Longitude					
1	2012	51°10'05"	93°42'07"	1249	Khovu-Aksy Stlmt	granite	57.2±6.1	–
2	2100	51°02'13"	93°59'10"	1315	Kyzyl-Erik River	diorite	69.9±4.2	–
3	2080	51°01'30"	93°33'43"	1664	Ulug-Sailyg River	plagiogranite	50.8±5.6	–
4	2206	50°59'20"	93°30'11"	1805	Ulug-Sailyg River	diorite	83.4±4.7	11.4±1.3 (41)
5	4545	50°56'06"	93°25'05"	1768	Kholy River	granite	44.7±4.6	–
6	3640	50°45'32"	93°22'16"	1225	Ak-Chira Stlmt	diorite	45.3±2.2	11.5±1.6 (43)
7	2223	50°43'23"	93°48'25"	1145	Despen River	granite	35.5±2.2	12.1±1.8 (43)
8	2224	50°43'52"	93°48'25"	1226	Despen River	granite	73.2±4.6	11.9±1.5 (51)
9	2225	50°44'35"	93°48'43"	1313	Despen River	granite	55.1±4.8	12.1±1.7 (47)
10	2226	50°45'14"	93°48'50"	1439	Despen River	granite	74.9±3.8	11.8±1.5 (58)
11	2227	50°45'50"	93°48'50"	1452	Despen River	granite	56.8±3.5	12.2±1.5 (50)
12	2228	50°46'23"	93°48'54"	1523	Despen River	granite	59.3±3.1	12.3±1.6 (53)
13	TV-57	50°37'31"	95°13'28"	1365	Samagaltay Stlmt	diorite	94.1±5.2	13.1±1.5 (60)
14	TV-58	50°38'14"	95°18'34"	1210	Samagaltay Stlmt	granodiorite	90.6±9.3	–
15	TV-41	50°26'22"	94°46'29"	1225	Tes-Khem River	tonalite	92.8±5.7	13.5±1.8 (100)
16	TV-50	50°28'31"	94°58'46"	1240	Tes-Khem River	diorite	87.7±4.9	13.9±1.6 (73)
17	TV-46	50°30'19"	94°44'46"	1010	Tes-Khem River	granodiorite	94.7±5.0	12.7±2.3 (64)
18	TV-56	50°17'43"	95°17'11"	1250	Moren–Erzin Stlmts	aplite	89.3±7.5	–
19	TV-55	50°17'28"	95°18'18"	1140	Moren–Erzin Stlmts	granite	80.8±7.2	–
20	TV-54	50°17'45"	95°17'10"	1270	Moren–Erzin Stlmts	granite	80.7±3.9	13.6±0.9 (100)
21	TV-38	50°12'58"	95°25'21"	1235	Erzin Stlmt	granite	83.1±3.6	13.7±1.3 (100)
22	TV-37	50°11'45"	95°36'24"	1385	Erzin Stlmt	gneiss	87.0±5.7	13.2±1.7 (100)
23	TV-36	50°11'08"	95°36'49"	1540	Erzin Stlmt	gneiss	93.8±4.3	13.5±2.1 (100)

Note. Apatite fission-track ages and mean track lengths ± standard deviation after [De Grave et al., 2014; Vetrov et al., 2022]. The number of measurements from which the mean track lengths were obtained is shown in parentheses.

of the most sensitive low-temperature geochronological methods for obtaining quantitative information on tectonic processes in the upper crustal conditions at time intervals from millions to hundreds of millions years. As well as in case of other thermochronological methods, the AFT analysis is a method of geological dating at which the preservation of U^{238} radioactive decay products is sensitive to high temperatures (higher than 120 °C). The temperature range for partial track annealing in apatite is constrained to an interval of ~60–120°C, which, according to geothermal gradient ~25 °C/km (typical foldbelts), corresponds to an upper crustal depth of ~2 km ~5 km [Wagner, Van den Haute, 1992]. This method is a good tool for reconstructing thermal history of the basement rocks over a long period of time (to ~200–150 Ma for the CAFB). In many cases, the low-temperature thermochronometers show the ages which are rarely related to the start time of isotopic activity. These ages often record thermal and tectonic processes reflecting the result of a long-term surface denudation rather than the formation ages of the rocks studied. Most of the AFT ages are "mixed", showing an integrated result of low-temperature thermal history in upper crustal conditions. Thermotectonic modeling based on the parameters, obtained from the AFT analysis, and thermal histories for certain samples makes it possible to visualize differential cooling history of basement rocks, their denudation, and instrumentally confirmed evolution of relief [Kohn et al., 2002; Vetrov et al., 2016].

Thermotectonic modeling implies drawing regional schemes for distribution of AFT parameters (AFT ages and mean track lengths) and a series of spatiotemporal images demonstrating the dynamics of basement rock cooling from 120 °C to temperatures of a modern surface, denudation chronology, and evolution of relief. The schemes for regional distribution of the AFT dating data allow visualizing a spatial inhomogeneity of the AFT parameters obtained and estimating the age of the oldest discrete tectonic event. The results of individual thermal histories for certain samples are represented as consecutive images of certain time intervals, showing the regional history of basement rock cooling [Gallagher, Brown, 1999; Kohn et al., 2002]. Whereas the results of individual thermal histories emphasize the detailed aspects of cooling histories for certain samples, the regional representation provides a quantitative assessment for an average basement denudation rate as a function of time. Geothermal gradient ~25 °C/km can be used to convert temperature values to quantitative estimations of the basement denudation volumes. Such approach allows the reconstruction of denudation chronology for each sample and uses the nearest neighbor interpolation to create a spatial grid for each time step.

This grid is then spatially integrated in subsequent time intervals to obtain the regional denudation chronology. This scheme satisfies the data obtained and involves weighting based on a spatial distribution of these sites to do interpolation. This method does not need smoothing and eliminates a general problem of indefinite characteristics in the interpolated field. A combination of the denudation model and the digital elevation model data provides a possibility of modeling the paleotopographic evolution. Paleotopography is assessed using a serial subtraction of the amount of material denuded in a certain period of time on the current surface with regard to isostatic equilibrium. The estimating of paleoheights, reconstructed during thermotectonic modeling, reflect only a passive response to denudation discharge and, for better reliability, can be supplemented with other parameters, for example, the data on sea-level change relative to the present-day Earth's surface or assessments of local deformation and/or thrust amplitudes [Kohn et al., 2005]. The present study deals with thermotectonic modeling for the Pre-Mesozoic basement of South Tuva from the AFT analysis data including 23 dates and 16 thermal histories [De Grave et al., 2014; Vetrov et al., 2022]. The AFT samples were taken from the Paleozoic magmatic and metamorphic rocks in the height interval 1000–1800 m along three profiles (Fig. 3), intersecting the main fault zones of South Tuva (Table 1).

The results obtained from analytical procedures are presented in Table 1 and Fig. 4. Thermal history modeling (see Fig. 2) was conducted using QTQt [Gallagher, 2012] and HeFTy [Ketcham, 2005], annealing equations [Ketcham et al., 2007], and Markov Chain Monte Carlo based inverse modeling. The details of analytical works and thermal history modeling techniques are reported in [De Grave et al., 2014; Vetrov et al., 2022]. The regional schemes of distribution of AFT parameters (Fig. 5) and series of spatiotemporal images are drawn using ArcMap and ArcScene tools algorithms (version 10.4.1) (Fig. 6, 7, 8). Cooling history of basement rocks (see Fig. 6) and denudation chronology (see Fig. 7) are presented in a two-dimensional format over the last 125 Ma at 25 Ma intervals. The evolution of relief is estimated using the SRTM data and represented in a three-dimensional format over the last 100 years at 25 Ma intervals (Fig. 8).

3. APPLICATION OF APATITE FISSION-TRACK ANALYSIS IN THE STUDY OF THE ROCKS OF SOUTH TUVA

The results of AFT analysis (AFT ages and mean track lengths) for the basement rocks of South Tuva are presented in Table 1. Generally, the AFT ages obtained are varying from the Late Cretaceous (94.7±5.0 Ma) to the Late Eocene (35.5±2.2 Ma). AFT ages from the basement rocks of South Tuva are somewhat younger than those from other northern segments of the CAFB [De Grave et al., 2009, 2011; Arzhannikova et al., 2013; Zhimulev et al., 2021; Vetrov et al., 2021b]. Note that the Cretaceous and Eocene ages were obtained at similar heights and, on the contrary, similar ages were obtained for the samples taken at different heights. For example, sample TV-46 was taken at an absolute height of 1010 m and yielded the Late Cretaceous (~95 Ma) AFT age, though sample TV-36, taken at a height of 1540 m, yields a similar age. As shown in Fig. 3, such data scattering is observed for three profiles intersecting the major fault zones of the study area. However, in case of the South Tannuola and Ubsunur–Bii-Khem fault

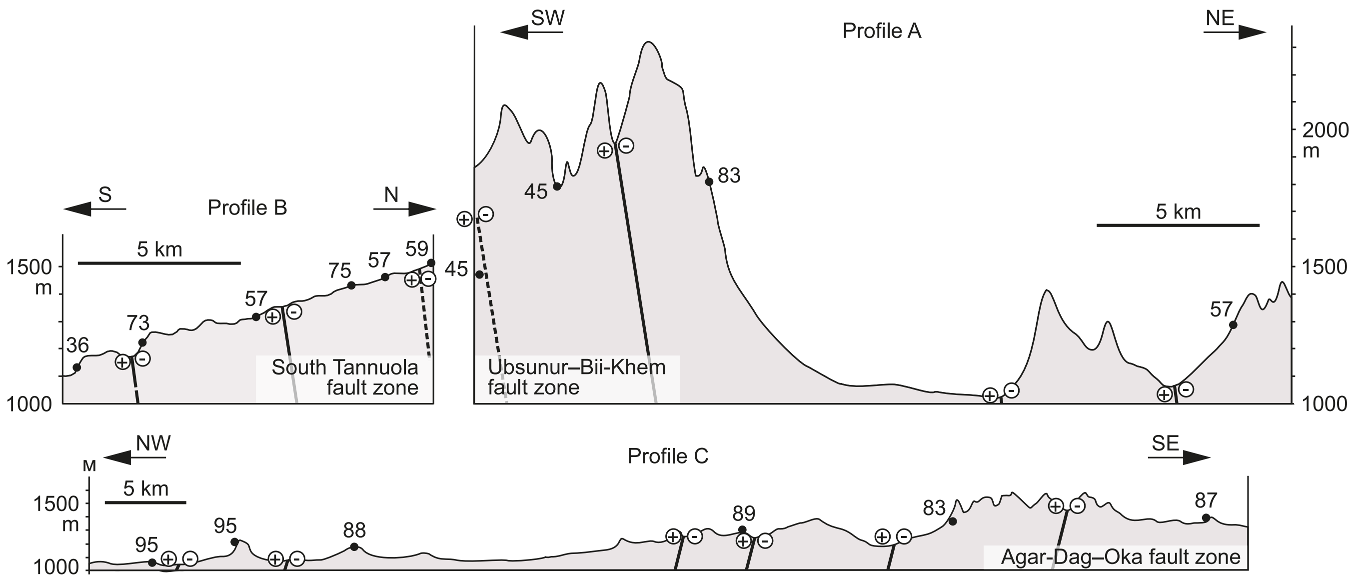

Fig. 3. Profiles intersecting the fault zones of South Tuva plotted using the results of AFT dating (Ma). The profile lines are shown by white dotted lines in Fig. 2.

zones, the "normal" vertical profile disturbance is related to activation of normal fault structures, and in case of the Agar-Dag–Oka fault zone – to that of reverse fault structures. It is obvious that the main activation phase of fault structures with different kinematics occurs at different times. To assess the periods of tectonic reactivation (fast cooling) and those of tectonic quiescence (slow cooling) from the AFT parameters, a comparison was made of the mean track lengths for each sample depending on its age (see Fig. 4). The mean track lengths for the basement rocks of South Tuva vary in the range of 11.4±1.3 to 13.9±1.6 μm. Most of the track length distributions are asymmetric mode [De Grave et al., 2014; Vetrov et al., 2022]. A relationship between the AFT age and the mean track length shows that the Pre-Mesozoic basement of South Tuva experienced several tectonic events. On this graph, the Cretaceous dates correspond to higher values of the mean track lengths, thus implying a rapid removal of basement rocks from the apatite partial annealing zone (ARAZ, temperature interval 120–60 °C). In its turn, a decrease in the AFT ages (from Cretaceous to Eocene) with a decrease in the mean track lengths (from 13.6 to 11.5 μm) testifies to a long-term presence of the analyzed rocks in the APAZ or even in deeper upper crustal zones.

Within the study area, 16 thermal histories of the Pre-Mesozoic basement rocks of South Tuva were modeled using Monte Carlo randomized algorithm. The obtained models of thermal histories show different rock cooling scenarios: one-, two-, three- and five-stage (see Fig. 2). One-stage cooling was modeled for samples 2223 and 2226 implying a moderate constant-rate basement rock cooling from 120 °C to the present-day surface temperatures. A two-stage model of thermal history obtained for samples TV-50 and TV-54 shows the Late Cretaceous (~100–80 Ma) stage of fast cooling from 120 °C to total annealing zone (TAZ, lower than 60 °C) with a subsequent subhorizontal behavior of the T-t trend curve up to the present.

The three-stage basement rock cooling is recorded in sample TV-46, demonstrating two fast cooling stages (125–100 Ma and the last 60 Ma), separated by the Cretaceous-Paleogene moderate cooling stage. Some other samples (for example, sample 3640), beside these three stages, recorded also two other, even older stages – Jurassic-Cretaceous (~190–140 Ma) slow cooling and Early Cretaceous (~140–125 Ma) stability or even insignificant heating.

4. THERMOTECTONIC MODELING RESULTS

Late Mesozoic and Cenozoic cooling history of the Pre-Mesozoic basement rocks. In order to perform the analysis of AFT parameters (AFT ages and mean fission-track lengths) obtained on the rocks of South Tuva, there is shown their regional distribution (see Fig. 5). This distribution demonstrated a high concentration of the Cretaceous (~90 to 80 Ma) dates in the eastern part of the study area (Sungilen upland) and that of the younger, Paleocene-Eocene (~60 to 45 Ma) dates in its western part (Tannuola range). The regional distribution of the mean track lengths, with the least lengths (11.6 to 12.0 μm) concentrated in the junction area between the South Tannuola and Ubsunur–Bii-Khem fault zones, correlates with the AFT age distribution. To make a generalization of different types of thermal histories, a series of images (see Fig. 6) was drawn to reflect a regional cooling history of the South Tuva basement rocks during their transportation to the

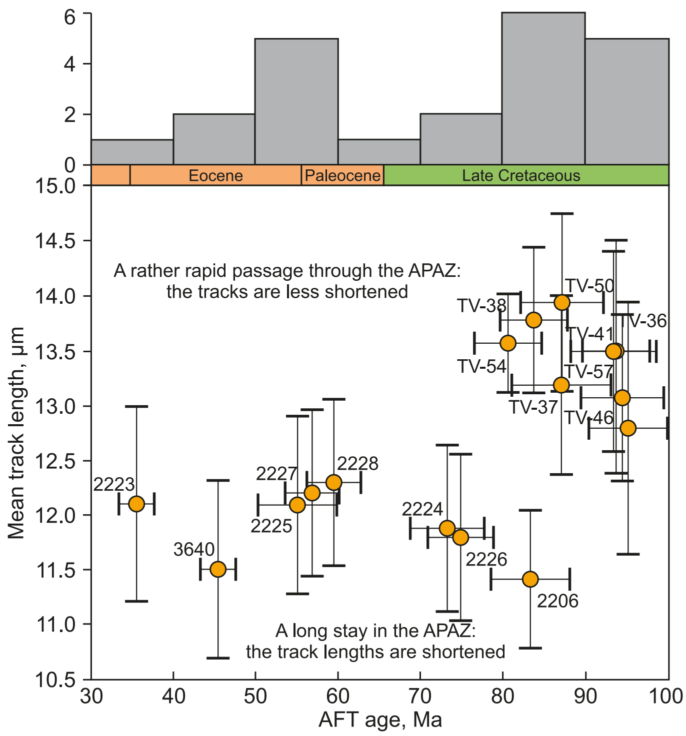

Fig. 4. Plot of AFT ages versus mean track lengths (bottom), frequency distribution of AFT ages (top).

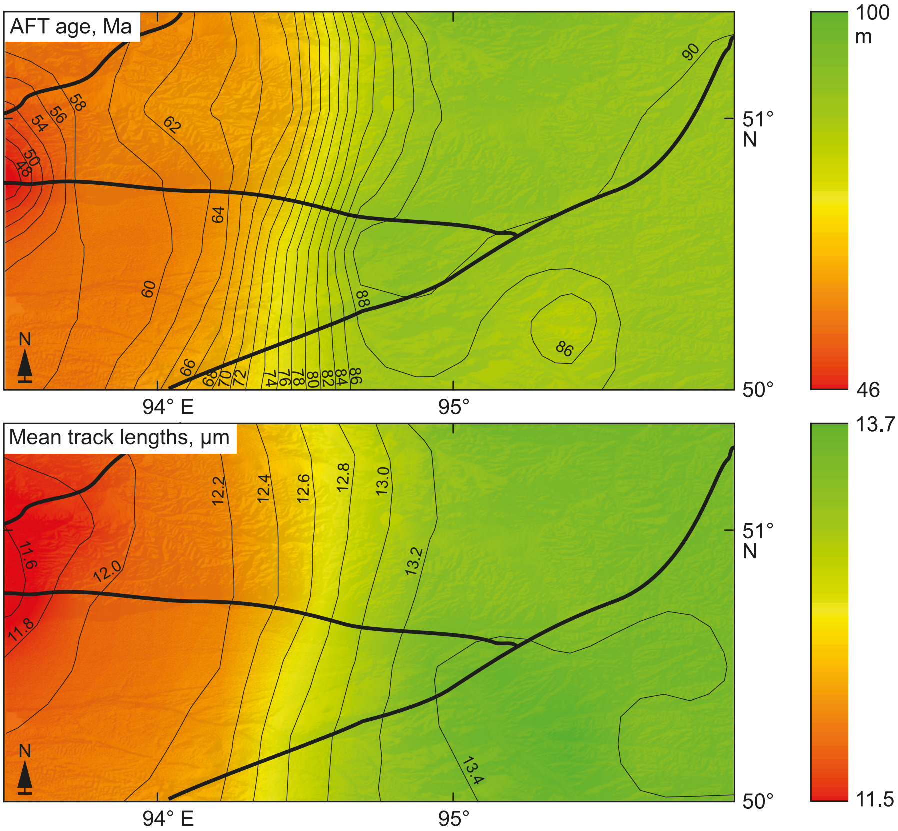

Fig. 5. Regional distribution of AFT ages (top, Ma) and mean fission-track lengths (bottom, μm) for the Pre-Mesozoic basement rocks of South Tuva.

surface through the upper crust. This image series implies the assumption of common trends in dynamically heterogeneous cooling of the South Tuva basement rocks. The most contrasting cooling of the area occurred in the Late Cretaceous (100–75 Ma) and Late Oligocene-Holocene (25–0 Ma). The Cretaceous-Paleogene (75–50 Ma) interval is characterized by a relatively stable position of paleoisotherms.

Late Mesozoic and Cenozoic denudation of the Pre-Mesozoic basement rocks. Differential basement surface cooling of South Tuva may result from uneven exhumation and denudation of the basement rocks due to different stages of tectonic activation of the major fault zones. To visualize the regional denudation events over the last 125 Ma, the image series shows denuded zones at intervals of 25 Ma within 0 to 2000 m (see Fig. 7). The change of areas with high volumes of denuded zones marks different stages of activation of the regional Paleozoic fault zones controlling the basement evolution of South Tuva. Regional models reveal somewhat high denudation rate (to 40 m/myr) of the South Tuva basement rocks in the junction area between the South Tannuola and Agar-Dag–Oka fault zones at the end of the Early Cretaceous (125–100 Ma). And at the same time denudation rates for the rest of South Tuva remained generally low (10 to 20 m/myr). In the Late Cretaceous (100–75 Ma), the rate of basement denudation increased (to 70 m/myr) in the eastern part of the study area mostly due to activation of the Agar-Dag–Oka fault zone. The Late Cretaceous – Early Paleogene (75–50 Ma) is characterized by some stability of denudation rates; at least the major fault structures of South Tuva were tectonically stable. A subsequent increase in the rate of basement denudation (to 40 m/myr against the background of 10–20 m/myr) for South Tuva occurred along the South Tannuola fault zones in the Late Paleogene (50–25 Ma). The Late Paleogene basement denudation and exhumation gave rise to coarse-grained sediment deposition of the Late Eocene Kurgak formation in the Ubsunur basin to the south of the South Tannuola fault zone. The denudational processes continued in the Neogene (25–0 Ma), having attained their maximum (to 50 m/myr) in the junction area between the South Tannuola and Ubsunur–Bii-Khem fault zones. Denudation rates are at the same time insignificant (15–20 m/myr) in the area controlled by the Agar-Dag–Oka fault zones. High rock denudation and exhumation rates of South Tuva in the Neogene are confirmed by the occurrence of continental molasse in the Ubsunur basin. The Late Neogene reactivation process of the South Tannuol and Ubsunur–Bii-Khem fault zones was going on during the Quaternary and continues to this day. This is evidenced by the concentration of epicenters of recent earthquakes with a magnitude of up to 7 and 3000–3500 years old earthquakes known within South Tuva [Ovsyuchenko, Butanayev, 2017].

Late Mesozoic and Cenozoic relief development history. Thermotectonic modeling based on the AFT analysis

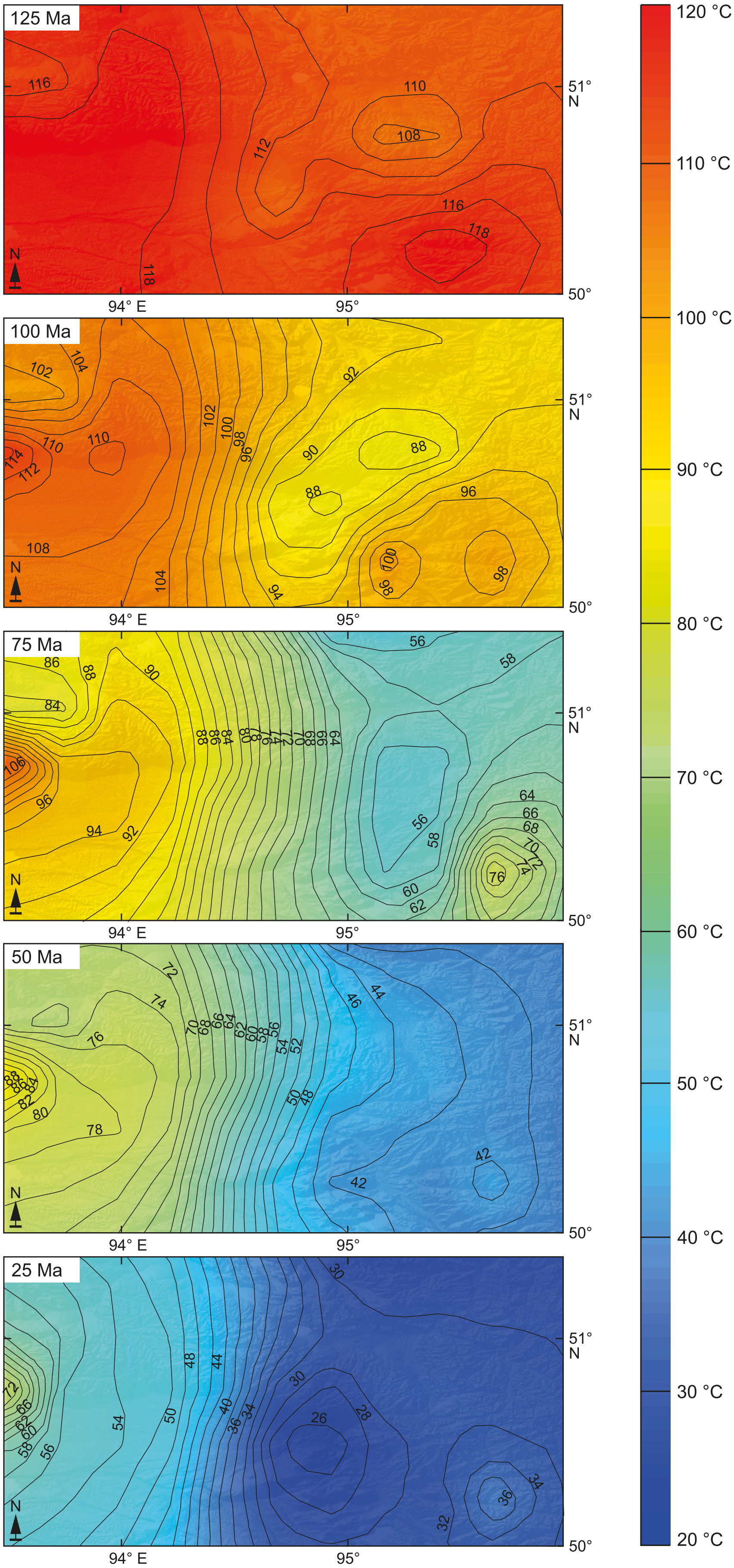

Fig. 6. Cooling history of the South Tuva basement for 125 million years.

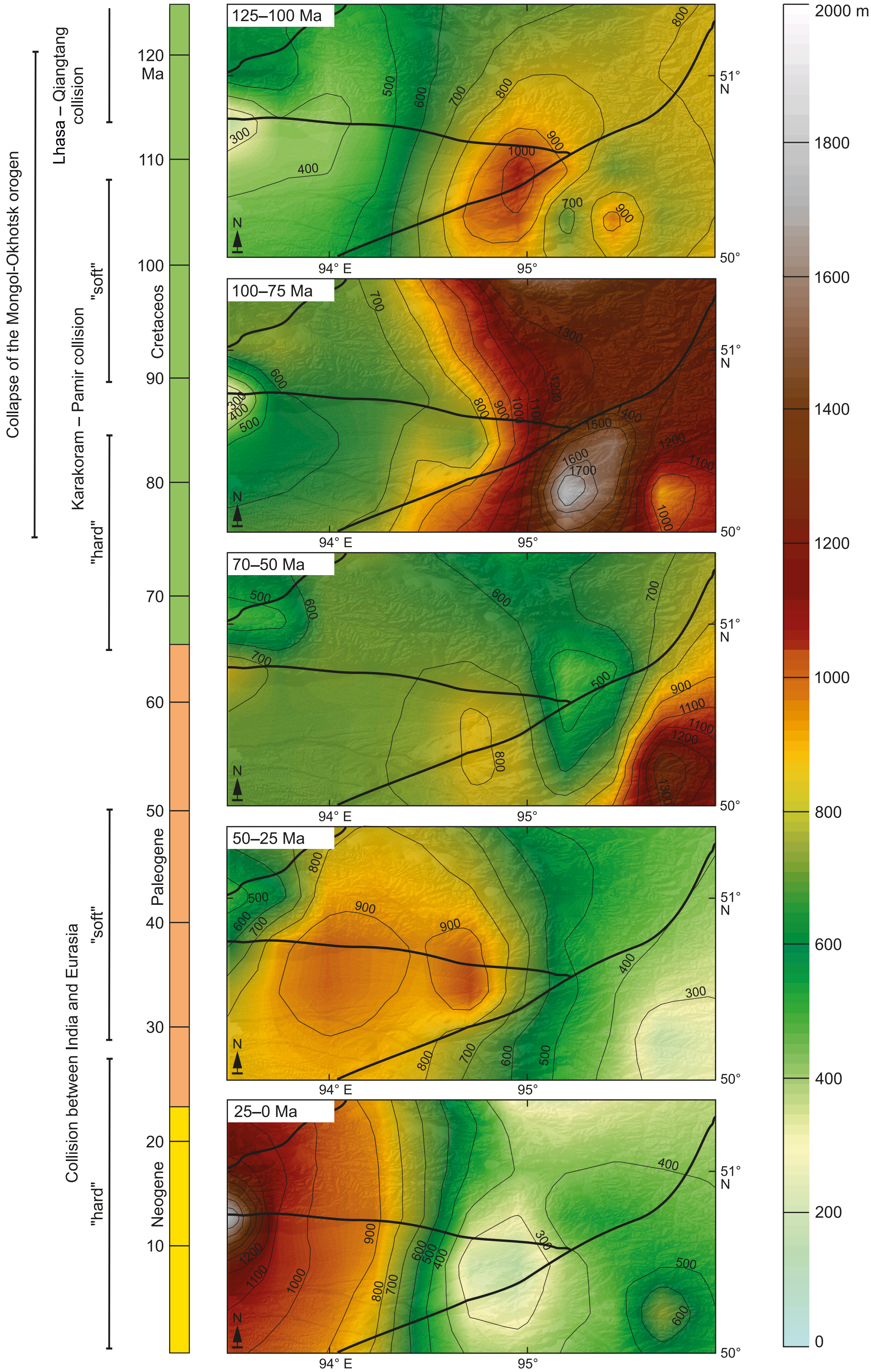

Fig. 7. Denudation chronology of the Pre-Mesozoic basement rocks of South Tuva. Shown on the left is the chronology of tectonic events at the southern and southeastern margins of Eurasia.

data, including thermal histories, allows estimating only the dynamics of vertical movements. However, this is one of the few methods capable of reconstructing an instrumentally reasonable long-term landscape evolution model. Fig. 8 shows a series of 3D relief images for five time slices over the last 100 Ma. Paleotopographic scheme of a 100 Ma time slice demonstrates that at the beginning of the Late Cretaceous South Tuva was an even surface with absolute heights up to 750 m. Then, at the end of the Late Cretaceous (75 Ma), against the background of global sea level rise, within South Tuva there occurred uplifted segments (near the present-say Sangilen upland) with absolute heights of 800 to 1200 m relative to the sea level of that time. The epicontinental sea basin (West Siberian), existed on the adjacent area at that time, was connected with the World Ocean and could serve as a denudation base [Novikov et al., 2019]. The Cretaceous-Paleogene stage (75–50 Ma) is characterized by an even rock denudation rate of South Tuva and the absence of any contrasting tectonic uplifts. At that time, in the northern regions of the CAFB, there occurred a peneplanation with the formation of weathering crusts due to climate warming [Dobretsov et al., 1996; Velichko, 1999]. Some increase in the heights on the paleotopographic scheme for a 50 Ma time slice, as compared to a 75 Ma time slice, can be caused by a 100–125 m sea level decrease in the Cretaceous-Paleogene (75–50 Ma). In the Late Paleogene (25 Ma) there was a moderately dissected relief with absolute heights of 500 to 1400 m, with a rise of the western part of the study area (present-day Tannuola range) started at the same time. The present-day orography of South Tuva was formed over the last 25 Ma. In that period of time there formed the highest mountain systems (for example, Tannuola range) which provided debris supply into the neighboring Ubsunur basin.

5. THE MESOZOIC AND CENOZOIC UPPER CRUSTAL TECTONIC PROCESSES IN SOUTH TUVA. DISCUSSION

Thermotectonic modeling for the upper crust of South Tuva, based on the AFT analysis data, demonstrates several Mesozoic-Cenozoic cooling episodes related to differential denudation and exhumation of the Pre-Mesozoic basement after its Late Paleozoic consolidation. It is considered that the denudation rate and, therefore, dynamics of basement tectonic uplift can be affected by a number of factors including tectonics, climate, and global sea-level fluctuations. In case of South Tuva, a regional differentiation of denudational history, related to uneven basement rock exhumation, can hardly be attributed to global sea-level drop/rise and climate changes. Therefore, the key role in the Mesozoic and Cenozoic history of geological evolution of the upper crust of South Tuva is played by tectonic factors. During the study of the Mesozoic and Cenozoic tectonomagmatic events of the Tuva segment of the CAFB, the assumption was made about active mantle-crust interaction therein [Yarmolyuk et al., 2001; Lebedev et al., 2001, 2016], which can be responsible for periodic activation of fault structures. However, the identified episodes of rock denudation and exhumation can hardly be explained by mantle plume activity beneath the basement of South Tuva. If vertical movements were caused by convection currents in the mantle, they would have occurred more widely and resulted in synchronous activation of different regional fault structures. Besides, the southern part of the study area – the Tuva segment of the CAFB – yielded no Mesozoic or Cenozoic magmatic formations which could be indicative of mantle plume activity beneath the lithosphere of South Tuva.

The episodes of tectonic activity of regional fault structures accompanied by rock denudation and exhumation of South Tuva could occur as a result of the Mesozoic and Cenozoic far-field tectonic effects on the southern and southeastern boundaries of Eurasia. An increase in denudation and basement tectonic uplift rates of South Tuva in the Early Cretaceous (120–100 Ma) could be due to far-field effects of (1) post-collisional lithospheric extension after the closure of the Mongol-Okhotsk Ocean and subsequent convergence between Siberia and Amuria [Yang et al., 2015; Jolivet et al., 2017], (2) collision of the Lhasa block against the southern margin of Eurasia [Kapp et al., 2007; Zhu et al., 2013, 2016] or (3) collision between the Karakoram and the Pamir (see Fig. 7). The Late Jurassic to Early Cretaceous interval after the closure of the Mongol-Okhotsk Ocean is characterized by an extensional tectonic regime [Zorin, 1999; Sklyarov et al., 1997; Donskaya et al., 2013; Sorokin et al., 2020], associated with gravitational collapse of the Mongol-Okhotsk orogen [Jolivet et al., 2017] at the southeastern margin of Eurasia. It is inferred that this event occurred almost simultaneously with the Lhasa–Qiangtang collision along the southern margin of Eurasia. After that there was a collisional process between the Karakoram and the Pamir, which preceded the main phase of the Late Cretaceous convergence between these blocks. All these tectonic events could result in Early Cretaceous (~125–100 Ma) basement denudation and exhumation of South Tuva, though it is difficult to estimate the contribution of each thereto.

In the Late Cretaceous (100–75 Ma), the Karakoram block moved northward and collided with the Pamir at the southern margin of Eurasia [Schwab et al., 2004]. The stress field, produced by the Karakoram–Pamir collision, propagated towards the northeast deep into the continent of Eurasia and caused reorganization of tectonic blocks of the CAFB and reactivation of thrust structures such as the Agar-Dag–Oka fault zone which resulted in basement exhumation of the eastern South Tuva at that time.

Subsequently, as a result of the closure of the Neo-Tethys Ocean, there was the Early Cenozoic Indo-Eurasian collision which gave rise to development of a wide orogeny in the south of the Eurasia continent [Yin, Harrison, 2000; Green et al., 2008]. This large-scale collision initiated a new episode of reactivation of numerous segments north of the southern margin of Eurasia and could initiate another episode of basement exhumation of South Tuva due to reactivation of large fault structures (such as South Tannuola and Ubsunur–Bii-Khem fault zones). The Late Paleogene (50–25 Ma) Indo-Eurasian collision initiated activation of

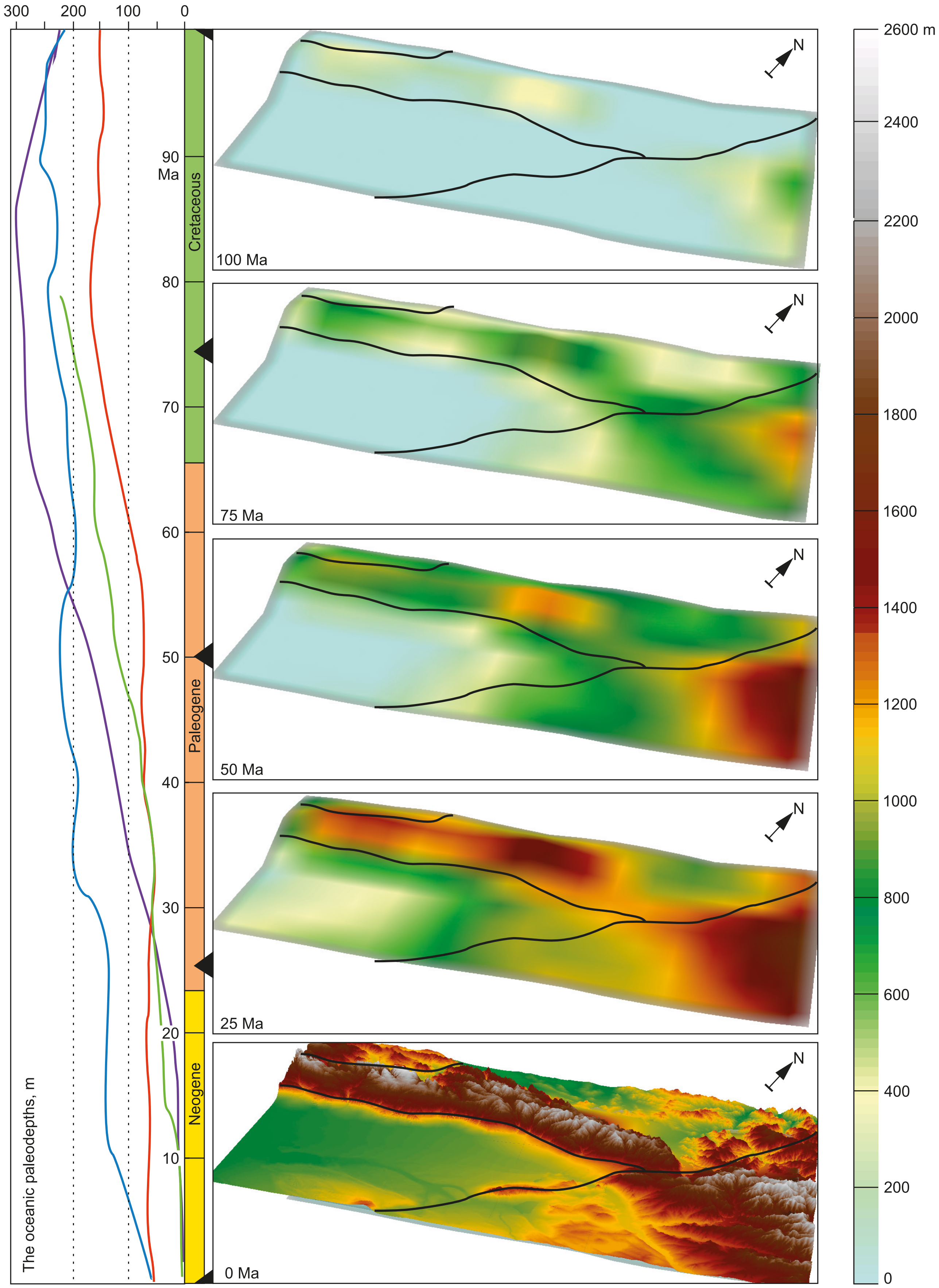

Fig. 8. Evolution of the landscape of South Tuva over 100 million years.
Purple, green, blue, and red lines on the left show the history of global sea level fluctuations after [Pitman, 1978; Kominz, 1984; Haq et al., 1987; Müller et al., 2008], respectively.

the South Tannuola and Ubsunur–Bii-Khem fault zones and a moderate-rate uplift of the eastern South Tuva. In the Neogene (25–0 Ma), this collision entered the main phase with the maximum basement uplift of South Tuva in the junction area of normal-fault zones. The obtained generalized regional denudation model yields a rough age estimate for the Neogene reactivation of fault structures and can always be refined based on the analysis of individual thermal histories modeled for individual samples. For example, according to individual thermal histories and a complex model of the Tannuola range [Vetrov et al., 2022], the maximum basement rock denudation of South Tuva began ~15 Ma in the junction area between the South Tannuola and Ubsunur–Bii-Khem fault zones.

6. CONCLUSION

Thermotectonic modeling, based on the apatite fission-track analysis data, visualized the Late Mesozoic – Cenozoic cooling history of the Pre-Mesozoic basement rocks in South Tuva, and provided a framework for reconstructing chronology and scale of denudation events and evolution of the paleorelief over the last 100 Ma. There was revealed a differential cooling of basement surface in South Tuva – the most contrasting cooling occurred 100–75 Ma and over the last 25 Ma. The analysis of denudational chronology also showed an uneven rock exhumation due to the process of staged reactivation of the main fault structures controlling tectonic evolution of the Pre-Mesozoic basement in South Tuva. In its turn, the activation of fault structures is caused by the far-field tectonic effects on the southern and southeastern margins of the Eurasia continent. The Early Cretaceous (~125–100 Ma) activation of the Agar-Dag–Oka thrust fault zone could result from the post-collisional processes after the convergence between Siberia and Amuria and/or a consecutive collision between the so called Cimmerian blocks (Lhasa, Qiangtang, Karakoram, Pamir). The Late Cretaceous (~100–75 Ma) tectonic processes in the south of Eurasia, such as the Karakoram-Pamir collision, intensified the activation of the Agar-Dag–Oka fault zone and caused an extensive basement exhumation in the eastern South Tuva at that time. The Cenozoic activation of the main fault zones in South Tuva is caused by a large-scale reorganization of tectonic blocks due to the Indo-Eurasian collision in the southern Eurasia continent. The main phase of this collision (25–0 Ma) is associated with the maximum basement uplift in South Tuva in the junction area between the South Tannuola and Ubsunur–Bii-Khem fault zones.

The reconstructed evolution of the paleorelief of South Tuva showed that at the beginning of the Late Cretaceous (~100 Ma) South Tuva was an even surface with heights to 750 m. At the end of the Late Cretaceous (75 Ma), the uplifted segments began to emerge, with absolute heights of 800 to 1200 m. In the Late Paleogene (25 Ma), there was a moderately dissected relief with absolute heights of 500 to 1400 m. The present-day relief of South Tuva was formed over the last 25 Ma, with the most intense transformations in the last 15 myr.

7. ACKNOWLEDGEMENTS

The authors express their gratitude to M.M. Buslov and an anonymous reviewer for their constructive comments which have been instrumental in improving the article.

8. CONTRIBUTION OF THE AUTHORS

Both authors made an equivalent contribution to this article, read and approved the final manuscript.

9. DISCLOSURE

Both authors declare that they have no conflicts of interest relevant to this manuscript.

10. REFERENCES

Arzhannikova A.V., Jolivet M., Arzhannikov S.G., Vassallo R., Chauvet A., 2013. The Time of the Formation and Destruction of the Meso-Cenozoic Peneplanation Surface in East Sayan. Russian Geology and Geophysics 54 (7), 685–694. https://doi.org/10.1016/j.rgg.2013.06.004.

Berzin N.A., Kungurtsev L.V., 1996. Geodynamic Interpretation of Altai-Sayan Geological Complexes. Russian Geology and Geophysics 37 (1), 63–81 (in Russian) [Берзин Н.А., Кунгурцев Л.В. Геодинамическая интерпретация геологических комплексов Алтае-Саянской области // Геология и геофизика. 1996. Т. 37. № 1. С. 63–81].

Buslov M.M., 2011. Tectonics and Geodynamics of the Central Asian Fold Belt: The Role of Late Paleozoic Large-Amplitude Strike-Slip Faults. Russian Geology and Geophysics 52 (1), 52–71. https://doi.org/10.1016/j.rgg.2010.12.005.

Buslov M.M., 2014. Terrane Tectonics of the Central Asian Orogenic Belt. Geodynamics & Tectonophysics 5 (3), 641–665 (in Russian) [Буслов М.М. Террейновая тектоника Центрально-Азиатского складчатого пояса // Геодинамика и тектонофизика. 2014. Т. 5. № 3. С. 641–665]. https://doi.org/10.5800/GT-2014-5-3-0147.

Buslov M.M., Geng H., Travin A.V., Otgonbaatar D., Kulikova A.V., Chen M., Stijn G., Semakov N.N., Rubanova E.S., Abildaeva M.A., Voitishek E.E., Trofimova D.A., 2013. Tectonics and Geodynamics of Gorny Altai and Adjacent Structures of the Altai-Sayan Folded Area. Russian Geology and Geophysics 54 (10), 1250–1271. https://doi.org/10.1016/j.rgg.2013.09.009.

Buslov M.M., Watanabe T., Fujiwara Y., Iwata K., Smirnova L.V., Safonova I.Yu., Semakov N.N., Kiryanova A.P., 2004. Late Paleozoic Faults of the Altai Region, Central Asia: Tectonic Pattern and Model of Formation. Journal of the Asian Earth Science 23 (5), 655–671. https://doi.org/10.1016/S1367-9120(03)00131-7.

De Grave J., Buslov M.M., Van den Haute P., Metcalf J., Dehandschutter B., McWilliams M.O., 2009. Multi-Method Chronometry of the Teletskoye Graben and Its Basement, Siberian Altai Mountains: New Insights on Its Thermo-Tectonic Evolution. Geological Society of London Special Publications 324, 237–259. https://doi.org/10.1144/SP324.17.

De Grave J., De Pelsmaeker E., Zhimulev F.I., Glorie S., Buslov M.M., Van den Haute P., 2014. Meso-Cenozoic Building of the Northern Central Asian Orogenic Belt: Thermotectonic

History of the Tuva Region. Tectonophysics 621, 44–59. https://doi.org/10.1016/j.tecto.2014.01.039.

De Grave J., Glorie S., Zhimulev F.I., Buslov M.M., Elburg M., Vanhaecke F., Van den Haute P., 2011. Emplacement and Exhumation of the Kuznetsk–Alatau Basement (Siberia): Implications for the Tectonic Evolution of the Central Asian Orogenic Belt and Sediment Supply to the Kuznetsk, Minusa and West Siberian Basins. Terra Nova 23 (4), 248–256. https://doi.org/10.1111/j.1365-3121.2011.01006.x.

Didenko A.N., Mossakovsky A.A., Pechersky D.M., Ruzhentsev S.V., Samygin S.G., Kheraskova T.N., 1994. Geodynamics of Paleozoic Oceans of Central Asia. Russian Geology and Geophysics 35 (7–8), 59–75.

Dobretsov N.L., 2003. Mantle Plumes and Their Role in the Formation of Anorogenic Granitoids. Russian Geology and Geophysics 44 (12), 1243–1261.

Dobretsov N.L., Buslov M.M., 2007. Late Cambrian-Ordovician Tectonics and Geodynamics of Central Asia. Russian Geology and Geophysics 48 (1), 71–82. https://doi.org/10.1016/j.rgg.2006.12.006.

Dobretsov N.L., Buslov M.M., Delvaux D., Berzin N.A., Ermikov V.D., 1996. Meso- and Cenozoic Tectonics of the Central Asian Mountain Belt: Effects of Lithospheric Plate Interaction and Mantle Plumes. International Geology Review 38 (5), 430–466. https://doi.org/10.1080/00206819709465345.

Dobretsov N.L., Buslov M.M., Vernikovsky V.A., 2003. Neoproterosoic to Early Ordovician Evolution of the Paleo-Asian Ocean: Implications to the Breakup of Rodinia. Gondwana Research 6 (2), 143–159. https://doi.org/10.1016/S1342-937X(05)70966-7.

Donskaya T.V., Gladkochub D.P., Mazukabzov A.M., Ivanov A.V., 2013. Late Paleozoic – Mesozoic Subduction-Related Magmatism at the Southern Margin of the Siberian Continent and the 150 Million-Year History of the Mongol-Okhotsk Ocean. Journal of Asian Earth Sciences 62, 79–97. https://doi.org/10.1016/j.jseaes.2012.07.023.

Gallagher K., 2012. Transdimensional Inverse Thermal History Modeling for Quantitative Thermochronology. Journal of Geophysical Research: Solid Earth 117 (B2), B02408. https://doi.org/10.1029/2011JB008825.

Gallagher K., Brown R.W., 1999. Denudation and Uplift at Passive Margins: The Record on the Atlantic Margin of Southern Africa. Philosophical Transactions of the Royal Society A. Mathematical Physical and Engineering Sciences 357 (1753), 835–859. https://doi.org/10.1098/rsta.1999.0354.

Gordienko I.V., 2004. Volcanism in Various Geodynamic Settings of the Central Asian Orogenic Belt. Lithosphere (3), 4–16 (in Russian) [Гордиенко И.В. Вулканизм различных геодинамических обстановок Центрально-Азиатского складчатого пояса // Литосфера. 2004. № 3. С. 4–16].

Gordienko I.V., 2019. Relationship between Subduction-Related and Plume Magmatism at the Active Boundaries of Lithospheric Plates in the Interaction Zone of the Siberian Continent and Paleoasian Ocean in the Neoproterozoic and Paleozoic. Geodynamics & Tectonophysics 10 (2), 405–457 (In Russian) [Гордиенко И.В. Связь субдукционного и плюмового магатизма на активных границах литосферных плит в зоне взаимодействия Сибирского континента и Палеоазиатского океана в неопротерозое и палеозое // Геодинамика и тектонофизика. 2019. Т. 10. № 2. С. 405–457]. https://doi.org/10.5800/GT-2019-10-2-0420.

Green O.R., Searle M.P., Corfield R.I., Corfield R.M., 2008. Cretaceous-Tertiary Carbonate Platform Evolution and the Age of the India-Asia Collision along the Ladakh Himalaya (Northwest India). The Journal of Geology 116 (4), 331–353. https://doi.org/10.1086/588831.

Haq B.U., Hardenbol J., Vail P.R., 1987. Chronology of Fluctuating Sea Levels since the Triassic. Science 235 (4793), 1156–1167. https://doi.org/10.1126/science.235.4793.1156.

Jolivet M., Arzhannikova N., Frolov A.O., Arzhannikov S., Kulagina N., Akulova V., Vassallo R., 2017. Late Jurassic – Early Cretaceous Paleoenvironment Evolution of the Transbaikal Basins (SE Siberia): Implications for the Mongol-Okhotsk Orogeny. Bulletin Societe Geologique de France 188 (1–2), 9. https://doi.org/10.1051/bsgf/2017010.

Kapp P., DeCelles P.G., Gehrels G.E., Heizler M., Ding L., 2007. Geological Records of the Lhasa–Qiangtang and Indo-Asian Collisions in the Nima Area of Central Tibet. Geological Society of American Bulletin 119 (7–8), 917–932. https://doi.org/10.1130/B26033.1.

Ketcham R.A., 2005. Forward and Inverse Modeling of Low-Temperature Thermochronometry Data. Reviews in Mineralogy and Geochemistry 58 (1), 275–314. https://doi.org/10.2138/rmg.2005.58.11.

Ketcham R.A., Carter A., Donelick R.A., Barbarand J., Hurford A.J., 2007. Improved Modeling of Fission-Track Annealing in Apatite. American Mineralogist 92 (5–6), 799–810. https://doi.org/10.2138/am.2007.2281.

Kohn B.P., Gleadow A.J.W., Brown R.W., Gallagher K., Lorencak M., Noble W.P., 2005. Visualizing Thermotectonic and Denudation Histories Using Apatite Fission-Track Thermochronology. Reviews in Mineralogy and Geochemistry 58 (1), 527–565. https://doi.org/10.2138/rmg.2005.58.20.

Kohn B.P., Gleadow A.J.W., Brown R.W., Gallagher K., O'Sullivan P.B., Foster D.A., 2002. Shaping the Australian Crust over the Last 300 Million Years: Insights from Fission Track Thermotectonic and Denudation Studies of Key Terranes. Australian Journal of Earth Science 49 (4), 697–717. https://doi.org/10.1046/j.1440-0952.2002.00942.x.

Kominz M.A., 1984. Oceanic Ridge Volume and Sea-Level Change an Error Analysis. In: J.S. Schlee (Ed.), Interregional Unconformities and Hydrocarbon Accumulation. American Association of Petroleum Geologists, p. 109–127. https://doi.org/10.1306/M36440C9.

Lebedev V.I., Cherezov A.M., Kuzhuget K.S., Lebedeva M.F., Lebedeva S.V., Cherezova O.S., Chupikova S.A., 2001. Geological Formations, Deep-Seated Geodynamics and Seismicity of the Inner Asia Terrains (Tuva and Northwestern Mongolia). In: The State and Exploration of Natural Resources of Tuva and Adjacent Regions of Central Asia. Geoecology of Natural Environment and Society. TuvIENR SB RAS, Kyzyl, p. 34–45 (in Russian) [Лебедев В.И., Черезов А.М., Кужугет К.С., Лебедева М.Ф., Лебедева С.В., Черезова О.С., Чупикова С.А. Геологические формации, глубинная геодинамика и сейсмичность террейнов Внутренней Азии (Тува и Северо-Западная Монголия) // Состояние и освоение природных ресурсов Тувы и сопредельных регионов Центральной Азии. Геоэкология природной среды и общества. Кызыл: ТувИКОПР СО РАН, 2001. С. 34–45].

Lebedev V.I., Duchkov A.D., Kamenskiy I.L., Chupikova S.A., Rychkova K.M., 2016. Seismogeology and Geotermica of the Territory of Tuva. Vestnik of Tuva State University. Natural and Agricultural Sciences 2, 112–126 (in Russian) [Лебедев В.И., Дучков А.Д., Каменский И.Л., Рычкова К.М., Чупикова С.А. Сейсмогеология и геотермика территории Тувы // Вестник Тувинского государственного университета. Естественные и сельскохозяйственные науки. 2016. Т. 2. С. 112–126].

Molnar P., Tapponnier P., 1975. Cenozoic Tectonics of Asia: Effects of a Continental Collision. Science 189 (4201), 419–426. https://doi.org/10.1126/science.189.4201.419.

Müller R.D., Sdrolias M., Gaina C., Roest W.R., 2008. Age, Spreading Rates, and Spreading Asymmetry of the World's Ocean Crust. Geochemistry, Geophysics, Geosystems 9 (4), Q04006. https://doi.org/10.1029/2007GC001743.

Novikov I.S., Zhimulev F.I., Vetrov E.V., Savelieva P.Yu., 2019. Mesozoic and Cenozoic Geologic History and Surface Topography of the Northwestern Altai-Sayan Area. Russian Geology and Geophysics 60 (7), 781–792. https://doi.org/10.15372/RGG2019054.

Ovsyuchenko A.N., Butanayev Y.V., 2017. Seismic History of the Altai-Sayan Region and the 2011–2012 Earthquakes in Tuva. The New Research of Tuva 1, 162–180 (in Russian) [Овсюченко А.Н., Бутанаев Ю.В. Сейсмическая история Алтае-Саянского региона и место в ней тувинских землетрясений 2011–2012 гг. // Новые исследования Тувы. 2017. Т. 1. С. 162–180]. https://doi.org/10.25178/nit.2017.1.11.

Pitman W.C., 1978. Relationship between Eustacy and Stratigraphic Sequences of Passive Margins. GSA Bulletin 89 (9), 1389–1403. https://doi.org/10.1130/0016-7606(1978)89<1389:RBEASS>2.0.CO;2.

Schwab M., Ratschbacher L., Siebel W., McWilliams M., Minaev V., Lutkov V., Chen F., Stanek K., Nelson B., Frisch F., 2004. Assembly of the Pamirs: Age and Origin of Magmatic Belts from the Southern Tien Shan to the Southern Pamirs and Their Relation to Tibet. Tectonics 23 (4), TC4002. https://doi.org/10.1029/2003TC001583.

Sengör A.M.C., Natal'in B.A., Burtman V.S., 1993. Evolution of the Altaid Tectonic Collage and Paleozoic Crustal Growth in Eurasia. Nature 364, 299–307. https://doi.org/10.1038/364299a0.

Sklyarov E.V., Mazukabzov A.M., Mel'nikov A.I., 1997. Complexes of Metamorphic Cores of the Cordillera Type. Publishing House of SB RAS, Novosibirsk, 182 p. (in Russian) [Скляров Е.В., Мазукабзов А.М., Мельников А.И. Комплексы метаморфических ядер кордильерского типа. Новосибирск: Изд-во СО РАН, 1997. 182 с.].

Sorokin A.A., Zaika V.A., Kovach V.P., Kotov A.B., Xu W., Yang H., 2020. Timing of Closure of the Eastern Mongol – Okhotsk Ocean: Constraints from U-Pb and Hf Isotopic Data of Detrital Zircons from Metasediments along the Dzhagdy Transect. Gondwana Research 81, 58–78. https://doi.org/10.1016/j.gr.2019.11.009.

Velichko A.A., 1999. The Common Features of the Cenozoic Landscape and Climate Changes in North Eurasia. In: Climate and Landscape Changes over the Last 65 Ma (Cenozoic: from Paleocene to Holocene). GEOS, Moscow, p. 219–233 (in Russian) [Величко А.А. Общие особенности изменений ландшафтов и климата Северной Евразии в кайнозое. Изменение климата и ландшафтов за последние 65 миллионов лет (кайнозой: от палеоцена до голоцена). М.: ГЕОС, 1999. С. 219–233].

Vetrov E.V., 2016. The Mesozoic and Cenozoic Thermotectonic Evolution of the Southeastern Altai from the Apatite Fission-Track Analysis Data. PhD Thesis (Candidate of Geology and Mineralogy). Moscow, 200 p. (in Russian) [Ветров Е.В. Эволюция термотектонических событий Юго-Восточного Алтая в позднем мезозое и кайнозое по данным трековой термохронологии апатита: Дис. ... канд. геол.-мин. наук. 2016. М., 200 с.].

Vetrov E.V., Buslov M.M., De Grave J., 2016. Evolution of Tectonic Events and Topography in Southeastern Gorny Altai in the Late Mesozoic – Cenozoic (Data from Apatite Fission Track Thermochronology). Russian Geology and Geophysics 57 (1), 95–110. https://doi.org/10.1016/j.rgg.2016.01.007.

Vetrov E.V., Chernykh A.I., Babin G.A., 2019. Early Paleozoic Granitoid Magmatism in the East Tannu-Ola Sector of the Tuvinian Magmatic Belt: Geodynamic Setting, Age, and Metallogeny. Russian Geology and Geophysics 60 (5), 492–513, https://doi.org/10.15372/RGG2019047.

Vetrov E.V., De Grave J., Kotler P.D., Kruk N.N., Zhigalov S.V., Babin G.A., Fedoseev G.S., Vetrova N.I., 2021a. Evolution of the Kolyvan-Tomsk Granitoid Magmatism (Central Siberia): Insights into the Tectonic Transition from Post-Collision to Intraplate Settings in the Northwestern Part of the Central Asian Orogenic Belt. Gondwana Research 93, 26–47. https://doi.org/10.1016/j.gr.2021.01.008.

Vetrov E.V., De Grave J., Vetrova N.I., 2022. The Tectonic Evolution Paleozoic Tannuola Terrane of Tuva in the Mesozoic and Cenozoic: Data of Fission-Track Thermochronology of Apatite. Geotectonics 56, 471–485 https://doi.org/10.1134/S0016852122040094.

Vetrov E.V., De Grave J., Vetrova N.I., Zhimulev F.I., Nachtergaele S., Van Ranst G., Mikhailova P.I., 2020. Tectonic History of the South Tannuol Fault Zone (Tuva Region of the Northern Central Asian Orogenic Belt, Russia): Constraints from Multi-Method Geochronology. Minerals 10 (1), 56. https://doi.org/10.3390/min10010056.

Vetrov E.V., De Grave J., Vetrova N.I., Zhimulev F.I., Nachtergaele S., Van Ranst G., Mikhailova P.I., 2021b. Tectonic Evolution of the SE West Siberian Basin (Russia): Evidence from Apatite Fission Track Thermochronology of Its Exposed Crystalline Basement. Minerals 11 (6), 604. https://doi.org/10.3390/min11060604.

Vladimirov V.G., Vladimirov A.G., Gibsher A.S., Travin A.V., Rudnev S.N., Shemelina I.V., Barabash N.V., Savinykh Ya.V.,

2005. Model of the Tectonometamorphic Evolution for the Sangilen Block (Southeastern Tuva, Central Asia) as a Reflection of the Early Caledonian Accretion-Collision Tectogenesis. Doklady Earth Sciences 405, 1159–1165.

Wagner G.A., Van den Haute P., 1992. Fission Track-Dating. Springer, Dordrecht, 285 p. https://doi.org/10.1007/978-94-011-2478-2.

Wang B., Cluzel D., Shu L., Faure M., Charvet J., Chen Y., Meffre S., de Jong K., 2009. Evolution of Calc-Alkaline to Alkaline Magmatism through Carboniferous Convergence to Permian Transcurrent Tectonics, Western Chinese Tianshan. International Journal of Earth Sciences 98, 1275–1298. https://doi.org/10.1007/s00531-008-0408-y.

Wilhem C., Windley B.F., Stampfli G.M., 2012. The Altaids of Central Asia: A Tectonic and Evolutionary Innovative Review. Earth-Science Reviews 113 (3–4), 303–341. https://doi.org/10.1016/j.earscirev.2012.04.001.

Windley B.F., Alexeiev D., Xiao W., Kröner A., Badarch G., 2007. Tectonic Models for the Accretion of the Central Asian Orogenic Belt. Journal of the Geological Society of London 164 (1), 31–47. https://doi.org/10.1144/0016-76492006-022.

Xiao W., Windley F., Allen B., Han C., 2013. Paleozoic Multiple Accretionary and Collisional Tectonics of the Chinese Tianshan Orogenic Collage. Gondwana Research 23 (4), 1316–1341. https://doi.org/10.1016/j.gr.2012.01.012.

Yang Y.-T., Song C.-C., He S., 2015. Jurassic Tectonostratigraphic Evolution of the Junggar Basin, NW China: A Record of Mesozoic Intraplate Deformation in Central Asia. Tectonics 34 (1), 86–115. https://doi.org/10.1002/2014TC003640.

Yarmolyuk V.V., Lebedev V.V., Sugorakova A.M., 2001. The Eastern Tuva Region of Recent Volcanism in Central Asia: Periods, Products and Types of Volcanic Activity. Journal of Volcanology and Seismology 3, 3–32 (in Russian) [Ярмолюк В.В., Лебедев В.И., Сугоракова А.М. Восточно-Тувинский ареал новейшего вулканизма Центральной Азии: этапы, продукты и характер вулканической активности // Вулканология и сейсмология. 2001. Т. 3. С. 3–32].

Yin A., Harrison T.M., 2000. Geologic Evolution of the Himalayan-Tibetan Orogen. Earth and Planetary Sciences Annual Review 28, 211–280. https://doi.org/10.1146/annurev.earth.28.1.211.

Zhimulev F.I., Vetrov E.V., Novikov I.S., Van Ranst G., Nachtergaele S., Dokashenko S.A., De Grave J., 2021. Mesozoic Intracontinental Orogeny in the Tectonic History of the Kolyvan'–Tomsk Folded Zone (Southern Siberia): A Synthesis of Geological Data and Results of Apatite Fission Track Analysis. Russian Geology and Geophysics 62 (9), 1006–1020. https://doi.org/10.2113/RGG20204172.

Zhu D.-C., Li S.-M., Cawood P.A., Wang Q., Zhao Z.-D., Liu S.-A., Wang L.-Q., 2016. Assembly of the Lhasa and Qiangtang Terranes in Central Tibet by Divergent Double Subduction. Lithos 245, 7–17. https://doi.org/10.1016/j.lithos.2015.06.023.

Zhu D.-C., Zhao Z.D., Niu Y., Dilek Y., Hou Z.Q., Mo X.X., 2013. The Origin and Precenozoic Evolution of the Tibetan Plateau. Gondwana Research 23 (4), 1429–1454. https://doi.org/10.1016/j.gr.2012.02.002.

Zonenshayn L.P., Kuzmin M.I., Natapov L.M., 1990. Tectonics of Lithospheric Plates of the USSR. Book 1. Nedra, Moscow, 328 p. (in Russian) [Зоненшайн Л.П., Кузьмин М.И., Натапов Л.М. Тектоника литосферных плит территории СССР. М.: Недра, 1990. Кн. 1. 328 с.].

Zorin Y., 1999. Geodynamics of the Western Part of the Mongolia-Okhotsk Collisional Belt, Trans-Baikal Region (Russia) and Mongolia. Tectonophysics 306 (1), 33–56. https://doi.org/10.1016/S0040-1951(99)00042-6.